Demonstration of a solid-state optical cooler: An approach to cryogenic refrigeration

Bradley C. Edwards[a)]
Los Alamos National Laboratory, Mail Stop D436, Los Alamos, New Mexico 87545

Johnny E. Anderson
Los Alamos National Laboratory, Mail Stop J569, Los Alamos, New Mexico 87545

Richard I. Epstein
Los Alamos National Laboratory, Mail Stop D436, Los Alamos, New Mexico 87545

Gary L. Mills and Allan J. Mord
Ball Aerospace and Technologies Corporation, P.O. Box 1062, Boulder, Colorado 80306-1062

(Received 6 July 1999; accepted for publication 3 September 1999)

We report the successful operation of an optical cooler system. This device achieved 48 °C of cooling from room temperature and a heat lift of 25 mW when it was pumped with 1.6 W of laser light. Its performance as a function of pump laser wavelength and chamber temperature agrees well with theoretical models. This device validates the physics needed for exploiting the laser cooling of solids to develop practical optical refrigerators. © *1999 American Institute of Physics.* [S0021-8979(99)08923-9]

INTRODUCTION

The basic principles for optical refrigeration, cooling by anti-Stokes fluorescence, have been discussed for many decades.[1] When nearly monochromatic radiation passes through certain condensed materials, the light is absorbed and reradiated at a higher frequency. Since the increase in the energy of the photons is supplied by thermal phonons in the material, the object cools. Though simple in principle, actually cooling by this process has proven difficult, since a myriad of processes can turn light into heat and mask the optical refrigeration effect.[2] Recently, optical refrigeration has been demonstrated in ytterbium-doped fluoride glass, Yb:ZBLAN,[3,4] and in laser dye solutions.[5,6] Several studies have investigated ytterbium-based glasses and crystals for their potential in optical refrigeration.[7,8] Two independent, theoretical studies found that Yb:ZBLAN could be used as the working material in an optical refrigerator that operates below 80 K with efficiencies comparable to those of small mechanical cryocoolers.[9,10] Optical refrigerators such as these would be valuable for cooling space-borne and ground-based radiation detectors and electronics. Since these are solid-state devices without any moving parts, liquids, gases, or thermal connections between the cold and warm stages, other than structural supports, they would be free of vibrations, mechanically robust, reliable, and represent a useful, alternative approach to cryogenic refrigeration.

In this article we describe the performance of our bench-top optical cooler which is a major step toward the Los Alamos Solid-State Optical Refrigerator, or LASSOR, described in Ref. 9, and pictured in Fig. 1. Whereas previous work has only dealt with the demonstration of cooling in specific materials, the work reported here implements the essential aspects of a design to utilize cooling materials in a practical application. The cooler described below consists of a chamber capable of absorbing the fluorescent radiation while having low thermal emissivity, a cooling element with mirrors for trapping the pump light, support structure, and a shadow region for connecting the temperature readout and any objects to be cooled. Pumping this device with 1.6 W of 1030 nm laser light, we found the temperature of the 6 g, Yb:ZBLAN cooling element dropped 48 °C from room temperature. This system converted 1.5% of the incident laser power into cooling power, a dramatic increase over previous studies which had efficiencies below 0.05%.[3–6] These results show that a Yb:ZBLAN-based optical cooler functions essentially as predicted by theoretical models,[9,10] validating the physics necessary to develop practical, cryogenic optical refrigerators.

EXPERIMENT

To test the basic principles of optical refrigeration, we constructed a device that embodied most of the features of the LASSOR;[9] the remaining steps are to attach a payload to the cooling element and use diode lasers to pump the system. Figure 2 shows a schematic of this unit. The cooling element, shown in gray, is a cylinder of Yb^{3+}-doped ZBLAN (12 mm diam by 10 mm long), which is mirrored on both ends; one mirror has a 150-μm-diam pinhole for admitting the pump radiation. Low-thermal-conductivity, 400-μm-diameter, optical fibers support the cooling element inside a copper chamber with internal dimensions of 13 mm length and 14 mm diam. The interior walls of this cooler chamber are coated to absorb the fluorescence while having a low emissivity at thermal wavelengths (3–20 μm). The entire cooler is placed in a large vacuum vessel to decrease the thermal conduction between the glass and cooler chamber.

a)Electronic mail: bcedwards@lanl.gov

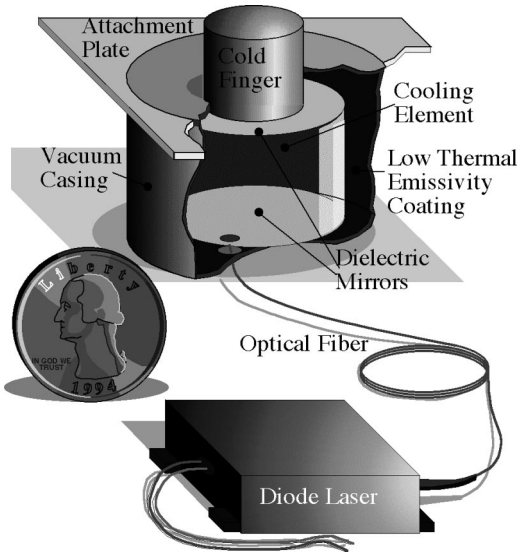

FIG. 1. Schematic of an optical cooler as described in Ref. 9. An efficient diode laser produces laser light of the appropriate frequency, and an optical fiber transmits this radiation to the cooling element. The cooling element is a cylinder of glass or crystal that exhibits high-quantum-efficiency anti-Stokes fluorescence and has high-reflectivity mirrors on both ends. The pump light enters the cooling element through a pinhole in one of the mirrors and is trapped in the cavity formed by the two mirrors. The cooling element absorbs the nearly collimated pump light and fluoresces isotropically. The fluorescence escapes through the sides of the cooling element and hits the inner surface of the heat-sunk chamber where it is absorbed. To minimize the radiative heat load on the cooling element, the inner surface of the chamber is prepared such that it has low emissivity at thermal wavelengths ($\sim 10\ \mu$m) while having high absorption at the wavelengths of the fluorescence ($\sim 1\ \mu$m). The item to be cooled, the ''load,'' is attached to the cooling element in the shadow region behind the second mirror (the one without the pinhole).

In our experiments the glass cylinder cools when the appropriate wavelength light from a Ti:sapphire laser is focused through the hole in the mirror. The cavity created by the mirrors on the ends of the cylinder traps the pump radiation until it is absorbed by the ytterbium. The fluorescence is absorbed by the chamber walls which carry away the energy from the pump laser and the heat removed from the glass. A liquid-flow, temperature-control system keeps the chamber at a constant temperature. Thermocouples glued to the glass, cooling element, and to the copper chamber measure their temperatures. We monitor the fluorescence with an optical fiber that passes through a sidewall of the cooler chamber.

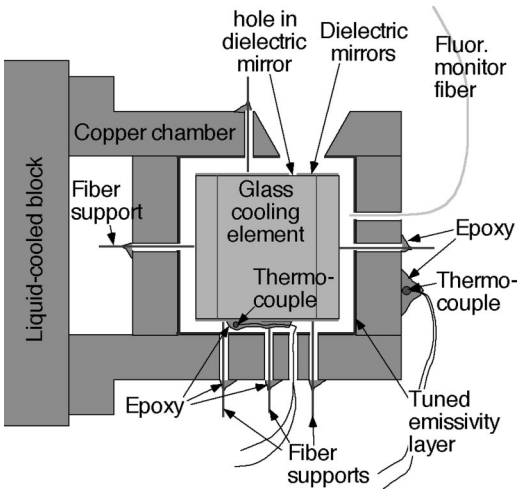

FIG. 2. Schematic of the bench-top, optical cooler setup.

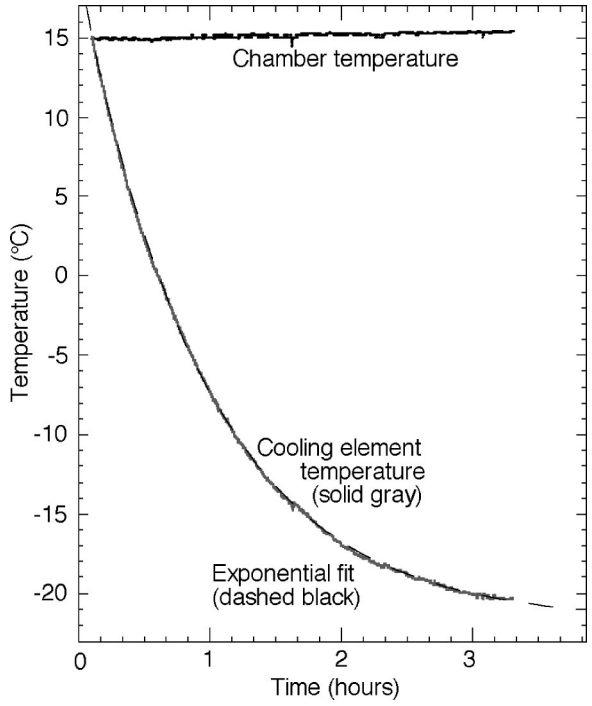

FIG. 3. Temperature measurements as the optical cooler is pumped by 1.55 W of 1030 nm laser light. The upper flat line is the temperature of the outer wall of the cooler chamber (see Fig. 2). The lighter gray curved line is the temperature of the cylindrical glass cooling element. The dashed black curve is the exponential fit to the cooling curve.

RESULTS

We pumped the optical cooler with up to 1.6 W of laser power at wavelengths between 950 and 1060 nm, while the cooler chamber was maintained at temperatures T_c between -27 and 22 °C. Figure 3 shows one cool-down experiment. The temperature of the cooler chamber is stable, and the glass temperature follows an exponential cooling curve with a time constant of $\tau = 65$ min. In this first set of experiments the maximum temperature drop we measured was 36.9 °C for a pump wavelength of 1032 nm, a pump power of 1.55 W, and the cooler chamber held at 22 °C. The *T*-type thermocouples that we used for all but the 48 °C measurement have possible systematic errors of ± 1 °C. For the measurement of the 48 °C drop we used a *K*-type thermocouple with a possible ± 2.2 °C systematic error. However, the consistency of the measurements of the temperatures of the cooling element and the chamber indicate that the uncertainties in the temperature changes are much smaller. With the laser power off, the cooling element has an equilibrium temperature that is between 0° and 1.2° warmer than the chamber, and this difference is anticorrelated with the chamber temperature. This difference may be due to the heating through the 3-mm-diam laser feed hole in the chamber.

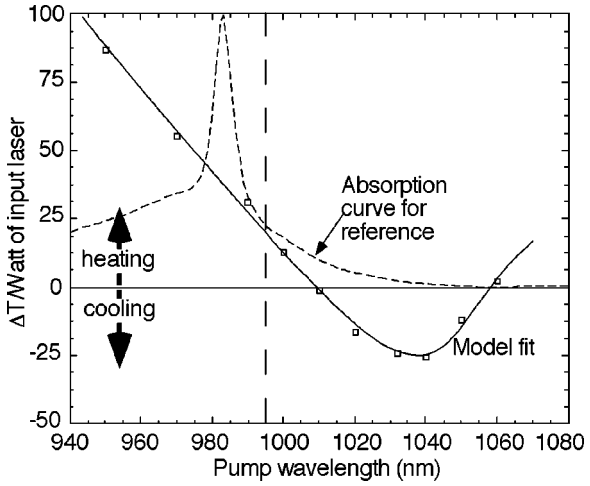

FIG. 4. Maximum temperature drop per watt of input laser power vs wavelength at 16 °C. The squares show the measured temperature drops, normalized to the pump power, for several pump wavelengths. The curve is a fit to the data using a model of the cooling element design and measured properties of Yb:ZBLAN (Refs. 8 and 9). The dotted line shows the absorption coefficient for Yb:ZBLAN at 27 °C. The vertical dashed line denotes the wavelength of the mean fluorescent energy.

Figure 4 shows the temperature change per watt of pump power for pump wavelengths between 950 and 1060 nm and the cooler chamber at 16 °C. The general shape of the curve is easily understood. At shorter pump wavelengths, where the incident photons have more energy than the fluorescent photons, the glass heats. For longer pump wavelengths, the less energetic photons cool the glass, and at still longer wavelengths, the absorption is so small that the cooler becomes ineffective. The solid curve represents a model of the cooler, discussed below, that includes various heating and loss mechanisms.

Figure 5 shows the effects of fixing the refrigerator chamber at different temperatures with a pump wavelength

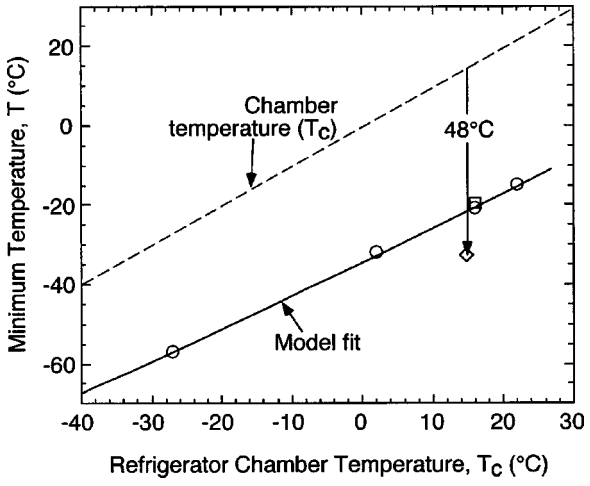

FIG. 5. Minimum temperature reached for a given cooler chamber temperature. The circles show the minimum temperature for 1.55 W of laser power at 1030 nm. For the data at 16 °C, the circle is the measured data for a pump power of 1.6 W, and we obtained the square by scaling the temperature drop by 1.55/1.6. The curves are model fits for which the thermal load is 47% conductive and 53% radiative at 16 °C. The diamond shows the 48 °C temperature drop that was achieved after the chamber was modified.

of 1030 nm. The circles give the minimum temperature attained. The pump power is 1.55 W, except for the measurements made with the chamber at 16 °C; in this case, the actual pump power is 1.60 W (shown by the circle) and the square represents the scaling of this measurement to 1.55 W. The decrease in temperature drop at lower chamber temperatures is due to an interplay between the temperature dependence of the ytterbium absorption and the heat load from the chamber; these effects are discussed below.

After this set of experiments, we modified the chamber to decrease the thermal load on the cooling element; these modifications are described in the next section. We then pumped the cooler with 1.60 W of laser power at 1030 nm and found that the temperature (T_c) of the cooling element decreased from 15 to −33 °C; i.e., a temperature drop of 48 °C. This result is shown by the diamond in Fig. 5.

DISCUSSION

The performance of the optical cooler is characterized by the magnitude of the temperature drop for different pump wavelengths and cooler chamber temperatures. The evolution of the temperature T of the cooling element is determined by energy conservation:

$$C\frac{dT}{dt} = -P_{\text{cool}} + P_{\text{heat}} + P_{\text{load}}, \tag{1}$$

where C is the heat capacity of the cooling element, P_{cool} is the cooling power, P_{heat} is heating that is proportional to the laser power, and P_{load} is the heating that is related to the temperature difference between the cooling element and its environment.

The temperature evolution, shown in Fig. 3, is governed by Eq. (1). The minimum cooling element temperatures $T_{\min}(\lambda)$ shown in Figs. 4 and 5 occur when $dT/dt = 0$. At this minimum temperature, P_{cool} equals $P_{\text{heat}} + P_{\text{load}}$. When the laser is off, $P_{\text{cool}} = P_{\text{heat}} = 0$ and $C\,dT/dt = P_{\text{load}}$. This allows measuring P_{load} directly during the warmup after an experimental run.

We now examine each of the terms in Eq. (1). The cooling from anti-Stokes fluorescence is

$$P_{\text{cool}} = P_{\text{abs}}\left(\frac{\lambda - \lambda_F}{\lambda_F}\right), \tag{2}$$

where $\lambda_F = 995$ nm is the wavelength that corresponds to the average photon energy of the fluorescence and P_{abs} is the pump radiation that is absorbed by the ytterbium ions. To find P_{abs}, note that pump light in the cooling element is attenuated as $\exp(-z/L)$, where z is the distance traversed and the mean-free-path L is given by $L^{-1} = \alpha + \beta$. Here, $\alpha(\lambda)$ is the absorption coefficient for the ytterbium (its spectrum at 27 °C is shown in Fig. 4), and β represents the other loss mechanisms, such as absorption on impurities, scattering, and leakage through the dielectric mirrors. We define the Q of the cooler element cavity as $Q = 1/(2\beta l)$, where l is the cavity length; i.e., $1/Q$ is the fraction of the pump light lost per round trip in the cooling element by processes other than absorption by ytterbium.

The absorbed power P_{abs} and the laser power P_{laser} incident on the cooling element are thus related by

$$P_{abs}(\lambda) = P_{laser} \int dz\, \alpha \exp\left(-\frac{z}{L}\right) = P_{laser}(\lambda)\left(1+\frac{1}{2\alpha l Q}\right)^{-1}. \quad (3)$$

For fluxes of the pump light comparable to the saturation flux, stimulated emission reduces the effective absorption coefficient.[4] The effects of saturation are negligible in the current experiments, and even in much more powerful optical refrigerators. Equation (3) shows that the precise value of $\alpha(\lambda)$ affects $P_{abs}(\lambda)$ only when the quantity $\alpha l Q$ is small. For this condition the saturation flux is >1 MW/cm^2, far above the peak flux density of the current experiment (<10 kW/cm^2).

There are three contributions to the P_{heat} term:

$$P_{heat} = \epsilon_1 P_{laser} + \epsilon_2 P_{abs} + \epsilon_3 N_{reflect} P_{laser}, \quad (4)$$

where $N_{reflect} \equiv 2Q/(1+2\alpha l Q)$ is the average number of reflections a photon makes with one of the dielectric mirrors, and the coefficients ϵ_i are model parameters. We identify the first term with heat produced by the laser interacting with absorbing material at the entrance pinhole hole. The second term could have contributions from nonradiative decay of the ytterbium excitations or from the escaping fluorescence interacting with absorbing substances on the surface of the glass or on the fibers and glue that support the cooling element. The third term, which varies with the distance a photon moves in the cooling element cavity, could arise from absorption of the pump light on the mirrors or by impurities in the glass.

The heat load P_{load} has two radiative terms and a conductive term:

$$P_{load} = \kappa_{r1}(T_c^4 - T^4) + \kappa_{r2}(T_v^4 - T^4) + \kappa_c(T_c - T), \quad (5)$$

where T_v is the temperature of the vacuum vessel holding the cooler chamber. The first term gives the radiative heat flow between the chamber and the cooling element. The second term describes the flow of radiation from the vacuum vessel to the cooling element through the 3-mm-diam hole in the cooler chamber used for the pump laser light. The third term is due to thermal conduction between the cooler chamber at T_c and the cooling element at T along the thermocouple wires and mechanical supports or through residual air in the chamber.

The radiation from the cooler chamber walls is mitigated by coating the walls with a film that has a low-thermal emissivity e_c so that[6]

$$\kappa_{r1} \cong \frac{e_c \sigma A_c}{1 + e_c(A_c/A - 1)}, \quad (6)$$

where σ is the Stefan–Boltzmann constant, A_c is the interior area of the cooler chamber, and A is the surface area of the cooling element, and we take the cooling element to be opaque to the thermal radiation. The term representing the heat leakage through the hole in the chamber is $\kappa_{r2} \cong \sigma A_{hole}$, where $A_{hole} \cong 0.08\,\text{cm}^2$ is the area of the hole.

Linearizing Eq. (5) and then solving Eq. (1) for the final equilibrium temperature of the cooling element, we find

$$T_c - T_{min} \propto P_{cool} - P_{heat} - \delta(T_v^4 - T_c^4), \quad (7)$$

where δ is a relatively small factor that does not depend on λ or T. The shape of the $T_{min}(\lambda)$, but not its the overall normalization, is thus determined by the wavelength dependence of $P_{cool} - P_{heat}$. Our best-model-fit curve to the data of Fig. 4 gives the following parameters: $Q \approx 120$, $\epsilon_1 \approx 1 \times 10^{-9}$, $\epsilon_2 \approx 0.014$, $\epsilon_3 \approx 1.9 \times 10^{-4}$. These are within the range of expectations, though the technology exists for improving all of these values.[9] The largest factor limiting the optical cooler's performance is the value $\epsilon_2 \approx 0.014$ representing the energy absorbed in the ytterbium and then converted to heat. In principle, this term could be due to nonradiative decay of the ytterbium ions; however, earlier measurements on the same and similar materials argue against this interpretation.[3] A more likely explanation is absorption of the fluorescence by surface contaminants and the thermocouple glued to the glass.

Linearizing Eq. (5) and using it with Eq. (1), we find for low laser power P_{laser} the cooling element relaxes to its equilibrium temperature with an exponential time constant $\tau \approx C/[\kappa_c + 4(\kappa_{r1} + \kappa_{r2})T_c^3]$. This expression agrees with the time constant $\tau \approx 65$ min derived from the data of Fig. 3 for $e_c \approx 0.1$ and $\kappa_c \approx 0.2$ mW/°C; which are near the expected values for the surface coating emissivity and the conductivity of the thermocouple wires and fiber supports.

The performance of the cooler at different cooler chamber temperatures, T_c, shown in Fig. 5, illustrates the balance of the optical refrigeration and the thermal load. On one hand, as the cooling element temperature falls, the absorption in the cooling tail declines[8] so that the absorbed power and cooling power decrease [see Eqs. (2) and (3)]. On the other hand, the heat load due to radiation from the cooler chamber walls falls with decreasing chamber temperature as T_c^3. The curve in Fig. 5 is the expected behavior if 47% of the thermal load on the cooling element at 16 °C is described by the conductive term in Eq. (5) and 53% is radiative.

Following the experiments discussed above, we modified the optical cooler chamber to reduce the conductive and radiative loads. The modifications included replacing the tuned emissivity layer on the ends of the cooler chamber with gold and reducing the size of each thermocouple wire from 1 to 0.5 mil. After these modifications, we pumped the cooler with 1.60 W of laser power at 1030 nm. The resulting temperature drop of 48 °C is a ~30% enhancement in cooling. When the laser was turned off at the minimum T, we found $dT/dt = 0.0091$ C/s, which gives a heat load of $P_{load} = 25$ mW. During warm up, the measured time constant τ was only 74 min. The model predicts that τ scales roughly as $T_c - T_{min}$ and should have been ~85 min.

CONCLUSIONS

The results presented here demonstrate the principle of optical refrigeration. The device we tested traps and absorbs the incident laser light at wavelengths from 950 to >1030 nm. The absorbed radiation removes heat from the cooling element by anti-Stokes fluorescence, and the escaping radia-

tion is absorbed in the heat-sunk chamber walls. Starting at 15 °C, we measured a maximum temperature drop of 48 °C. The performance of the current device is primarily limited by the ~2 W laser source used in these experiments. The Los Alamos Solid-State Optical Refrigerator concept[9] envisions a cryocooler driven by efficient, high-power diode lasers (~100 W). With the use of more powerful lasers and improvements in the mirroring and processing of the cooler elements, an efficient, compact, all solid-state cryocooler should be possible. The work reported here has found no apparent barriers to the implementation of a practical, optical refrigerator operating at cryogenic temperatures. Such devices would have wide applications in space-based and terrestrial radiation detectors and could enable the commercialization of electronics using high-temperature superconductor components.

ACKNOWLEDGMENTS

This work was conducted under the auspices of DOE and supported in part by IGPP/LANL and by Ball Aerospace and Technologies Corp. internal funds. The authors thank Charles Wilkerson, Melvin Buchwald, Don Casperson, Alan Gibbs, and Mary Cisper for their help and advice during this project and William Kiehl for commenting on an early version of the manuscript.

[1] P. Pringsheim, Z. Phys. **57**, 739 (1929); L. Landau, J. Phys. (Moscow) **10**, 503 (1946); A. Kastler, J. Phys. Radium **11**, 255 (1950); *Advances in Quantum Electronics*, edited by S. Yatsiv (Columbia University Press, New York, 1961).
[2] T. Kushida and J. E. Geusic, Phys. Rev. Lett. **21**, 1172 (1968); H. Gauck, T. H. Gfroerer, M. J. Renn, E. A. Cornell, and K. A. Bertness, Appl. Phys. A: Mater. Sci. Process. **64A**, 143 (1997).
[3] R. I. Epstein, M. I. Buchwald, B. C. Edwards, T. R. Gosnell, and C. E. Mungan, Nature (London) **377**, 500 (1995); C. E. Mungan, M. I. Buchwald, B. C. Edwards, R. I. Epstein, and T. R. Gosnell, Phys. Rev. Lett. **78**, 1030 (1997); Appl. Phys. Lett. **71**, 1458 (1997); T. R. Gosnell, Opt. Lett. **24**, 1041 (1999).
[4] X. Lou, M. D. Eisaman, and T. R. Gosnell, Opt. Lett. **23**, 639 (1998).
[5] J. L. Clark and G. Rumbles, Phys. Rev. Lett. **76**, 2037 (1996); G. Rumbles and J. L. Clark, *ibid.* **77**, 2841 (1996); C. Zander and K. H. Drexhage, in *Advances in Photochemistry* (Wiley, New York, 1995), Vol. 20, p. 59.
[6] J. L. Clark, P. F. Miller, and G. Rumbles, J. Phys. Chem. **102**, 4428 (1998).
[7] A. E. Montoya, J. A. Sanzgarcia, and L. E. Bausa, Spectrochim. Acta A **54**, 2081 (1998); J. C. Fajardo, G. H. Sigel, Jr., B. C. Edwards, R. I. Epstein, T. R. Gosnell, and C. E. Mungan, J. Non-Cryst. Solids **213**, 95 (1997); M. T. Murtagh, G. H. Sigel, J. C. Fajardo, Jr., B. C. Edwards, and R. I. Epstein, *ibid.* (in press); C. E. Mungan, B. C. Edwards, R. I. Epstein, T. R. Gosnell, and M. I. Buchwald, Mater. Sci. Forum **239**, 501 (1997).
[8] G. Lei, J. E. Anderson, M. I. Buchwald, B. C. Edwards, R. I. Epstein, M. T. Murtagh, and G. H. Sigel, Jr., IEEE J. Quantum Electron. **34**, 1839 (1998).
[9] B. C. Edwards, M. I. Buchwald, and R. I. Epstein, Rev. Sci. Instrum. **69**, 2050 (1998).
[10] G. Lamouche, P. Lavallard, R. Suris, and R. Grousson, J. Appl. Phys. **84**, 509 (1998).